

Potent and Preferential Degradation of CDK6 via Proteolysis Targeting Chimera Degraders

Shang Su,^{†,‡,⊥} Zimo Yang,^{‡,⊥} Hongying Gao,^{†,‡} Haiyan Yang,[†] Songbiao Zhu,[§] Zixuan An,[†] Juanjuan Wang,[†] Qing Li,^{||} Sarat Chandralapaty,^{||} Haiteng Deng,[§] Wei Wu,^{*,†,⊥} and Yu Rao^{*,‡,⊥}

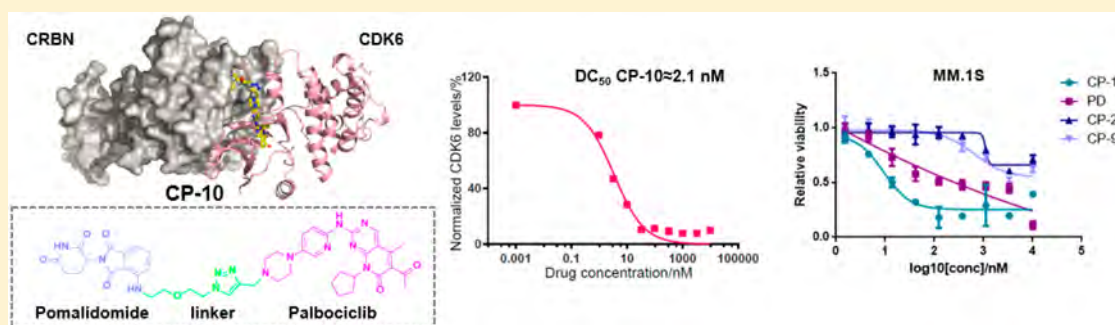
[†]MOE Key Laboratory of Protein Sciences, School of Life Sciences, Tsinghua University, Beijing 100084, P. R. China

[‡]MOE Key Laboratory of Protein Sciences, School of Pharmaceutical Sciences, MOE Key Laboratory of Bioorganic Phosphorus Chemistry & Chemical Biology, Tsinghua University, Beijing 100084, P. R. China

[§]MOE Key Laboratory of Bioinformatics, School of Life Sciences, Tsinghua University, Beijing 100084, P. R. China

^{||}Human Oncology and Pathogenesis Program, Memorial Sloan Kettering Cancer Center (MSKCC), New York, New York 10065, United States

S Supporting Information



ABSTRACT: A focused PROTAC library hijacking cancer therapeutic target CDK6 was developed. A design principle as “match/mismatch” was proposed for understanding the degradation profile differences in these PROTACs. Notably, potent PROTACs with specific and remarkable CDK6 degradation potential were generated by linking CDK6 inhibitor palbociclib and E3 ligase CRBN recruiter pomalidomide. The PROTAC strongly inhibited proliferation of hematopoietic cancer cells including multiple myeloma and robustly degraded copy-amplified/mutated forms of CDK6, indicating future potential clinical applications.

■ INTRODUCTION

Cell cycle regulation is one of the vital and housekeeping activities in most types of the cells.¹ Cyclin-CDK dual complexes are the major driving machinery for cell cycle progression.¹ Among the CDKs, CDK6 plays a significant role in cell cycle entrance and is frequently overexpressed or hyperactivated in cancer samples.² Therefore, small molecule inhibitors of CDK6 have been officially approved or clinically tested to act against cancers including breast cancer, lymphoma, and multiple myeloma.^{3–5} However, overexpression of CDK6, instead of its close homolog CDK4, induced by gene amplification or loss of FAT1 gene functions has been reported to be correlated to CDK4/6 inhibitor resistance in breast cancer cell lines and patient samples (Figure 1A).^{6,7} Moreover, point mutation of CDK6 could possibly result in attenuation of drug binding affinity or hyperactivation of CDK6, though not yet reported in clinical samples (Figure 1A).^{8,9} Thus, there is an urgent need to develop a practical strategy against CDK6-centered malignancy.

PROTAC (proteolysis targeting chimera) is an emerging chemical biology approach for targeted protein depletion by

exploiting the intracellular ubiquitin–proteasome system.¹⁰ A typical PROTAC molecule is bifunctional by combining a target-selective ligand and a specific E3 ligase recruiting ligand via a linker.¹¹ The resulting PROTAC could thus recruit the E3 ligase onto target protein and induce the ubiquitination and protein degradation via the proteasome (Figure 1B).^{11,12} The concept of targeted protein degradation was first proved by the groups of Crews and Deshaies in 2001 and was later successfully applied in multiple targets with different subcellular localizations, especially in hijacking cancer-related kinases.^{13–26} Notably, overexpressed BRD4 and drug-resistant mutated form of BTK and AR, which have been implicated in several different cancers, could be efficiently degraded through the PROTAC technique.^{15–17,27,28} These studies present the PROTAC technique as a promising alternative approach against cancer. Although this field has observed tremendous achievements in recent years, there is still a vast amount of challenges for PROTAC design to overcome. Various factors

Received: May 29, 2019

Published: July 22, 2019

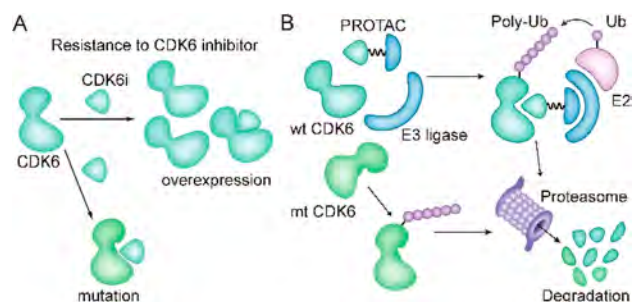


Figure 1. Resistance to CDK6 inhibitor and PROTAC technique for overcoming resistance. (A) Mechanisms for CDK6-centered resistance to CDK6 inhibitors. CDK6i is CDK6 inhibitor. Overexpression here indicates CDK6 overexpression resulting from CDK6 gene amplification or upstream FAT1 loss. Mutation here implies potential point mutation that hampers binding affinity of CDK6 inhibitor. (B) Induced degradation of wild type (wt) and mutated (mt) CDK6 proteins by PROTAC. E3 ligase is recruited to the proximity of target protein CDK6 and mediates polyubiquitination of CDK6, which is then processed into proteasome for degradation.

including ligand binding affinity, linker, spatial orientation, E3 ligase ligand, and cell permeability play vital roles in the functional capacity of PROTAC. Therefore, how these factors cooperate and function is a significant scientific issue to resolve. We selected CDK6 as the primary target to discuss how these critical factors are involved in the functional readout of successful PROTACs. We also propose that the resulting PROTAC molecules hold potential advantages over parental inhibitors in certain contexts with clinical significance, for example, specific subtype of cancers and intrinsic or acquired resistance caused by target (here as CDK6) overexpression or mutation (Figure 1B).

In this study, we report the design and synthesis of CDK6-targeting degraders using PROTAC strategy. These PROTACs could efficiently and specifically degrade CDK6 in low concentrations. More importantly, our newly designed PROTACs also significantly induced the degradation of mutant CDK6. Furthermore, our PROTAC molecules strongly inhibited proliferation of multiple myeloma, leukemia, and mantle cell lymphoma cells. These data demonstrate the significance and potential for developing PROTAC-based therapeutic molecules.

RESULTS AND DISCUSSION

On the basis of the literature^{14,26,29} and our previous experiences,^{17–19} we hypothesized that the degradation strength or efficiency of a certain PROTAC molecule was at least dictated by the following three major factors: the linker length, the spatial orientation of the target and the E3 ligase upon PROTAC conjugation, and binding affinity between PROTAC and its target. The success or failure of PROTAC is decided by the “match” or “mismatch” between PROTAC, E3 ligase, and target. Therefore, we applied various CDK6-targeting compounds, distinct E3 ligases, and multiple types of linker in PROTAC design. Specifically, we chose the three FDA-approved CDK4/6 inhibitors (palbociclib, ribociclib, and abemaciclib) which possess strong binding affinity but different terminal orientation to target CDK6.³⁰ The common terminal piperazine in the inhibitors from palbociclib, ribociclib, and abemaciclib stretched into solvent via distinct angles³¹ (Figure 2A).

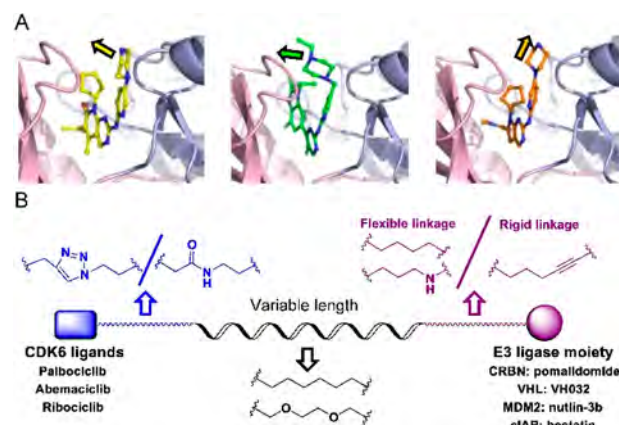
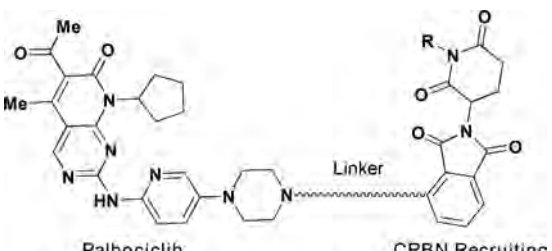


Figure 2. Design of CDK6-targeting PROTACs: (A) superimposed complex of CDK6 with palbociclib (yellow, PDB code 2euf), abemaciclib (green, PDB code 5l2s), ribociclib (orange, PDB code 5l2t); (B) representative structures of designed PROTACs library. Models were prepared with Pymol.

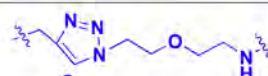
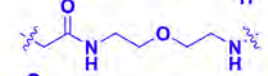
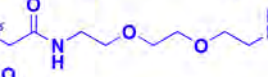
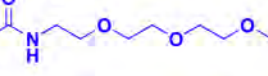
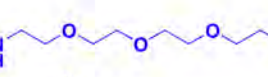
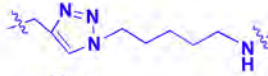

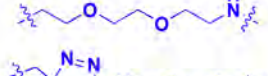



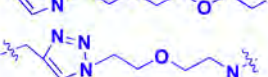

For palbociclib and abemaciclib, their piperazine moieties both stretch into the solvent horizontally, with slight deviation to N-terminal β -sheet of CDK6. In contrast, the terminal piperazine ring of ribociclib is farther from the solvent zone and folds toward the C-terminal α -helix. This may determine the overall rough spatial directions of derived PROTACs. Nonetheless, the aminopyrimidine stretches into the pocket and forms pivotal hydrogen bonds with surrounding amino acids to stabilize the complexes.³¹ The NH group in piperazine of palbociclib is exposed to the solvent, making it the most suitable site for attachment of linkers without disrupting critical binding interactions.^{31,32} Meanwhile, linking groups at the E3 ligase end can also profoundly affect the interacting angle between CDK6 and ligase, prompting us to introduce flexible and rigid groups, such as alkyl and alkyne, into the CRBN recruiting moiety pomalidomide. Additionally, nutlin-3b, VH032, and bestatin were also applied as recruiting moiety for E3 ligase MDM2, VHL, and cIAP, respectively, for the reason that we could not predict which ligase matches or mismatches with CDK6.^{30,33} Integrating the above principles, we designed and constructed a small focused library containing different types of PROTACs (Figure 2B and Table S1). For control, we also synthesized two negative control PROTAC molecules named CP-9 and CP-23 (corresponding to CP-2 and CP-10, respectively) by ethylation of pomalidomide end, thus blocking the binding between pomalidomide and CRBN and abrogating CDK6 ubiquitination.³³

We evaluated the degradation potential of all the designed CDK6-targeting PROTACs by in vitro assays (summarized in Tables 1 and 2; see also Figure S2). Interestingly, we found that CDK6 proteins were degraded only when PROTAC recruited CRBN but not the other three E3 ligases (Figure 3A,B). The degradation of CDK4 was less significant compared to CDK6 even though the target-binding molecules were believed to target both CDKs at similar potency, which will be discussed later. And again, CDK4 degradation was only observed in samples treated with CRBN-recruiting PROTACs. We ruled out the possibilities of E3 ligase deficiency and cell context specificity because the U251 glioblastoma cells express all these E3 ligases and the somehow CRBN-preference in CDK6 degradation was also observed in medullablastoma cell line DAOY (Figure S1). In theory, updating E3 recruiting

Table 1. Structures and DC_{50} Values for PROTACs Derived from Palbociclib and Pomalidomide^a


Palbociclib structure: A pyrimidine ring substituted with two methyl groups and a cyclopentyl group, connected via a pyridine ring to a piperazine ring, which is further connected to a linker.

CRBN Recruiting structure: A benzimidazole core with a variable R group, connected to a linker.

Compounds	Linker	R	DC_{50}/nM CDK6	DC_{50}/nM CDK4
CP-10		H	2.1	>100
CP-5		H	1.1	>100
CP-6		H	24.2	>100
CP-7		H	14.3	>100
CP-8		H	31.0	>100
CP-13		H	5.3	>100
CP-14		H	10.6	>100
CP-15		H	1.6	>50
CP-16		H	1.7	>50
CP-21		H	81.6	>100
CP-22		H	86.8	>100
CP-9		CH ₂ CH ₃	ND	ND
CP-23		CH ₂ CH ₃	ND	ND

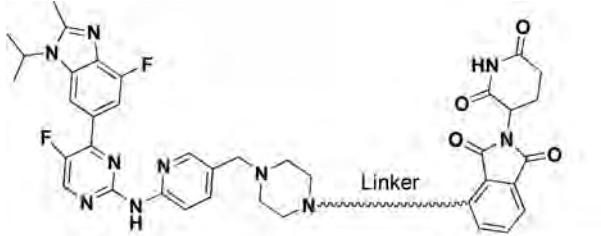
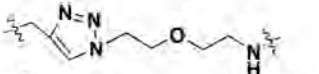
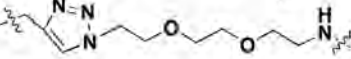
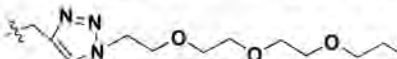

^aND indicates no degradation.

ligand potency can enhance the degradation potential of PROTAC; for example, introducing cIAP ligands with more potency than bestatin may facilitate CDK6 degradation. However, previous successful target degradation by PROTACs harboring the same ligands we used suggested that the CRBN preference we observed in this study could be more on the intrinsic/PROTAC-induced substrate selectivity of E3 ligases, which needs future investigation. Among the CRBN-recruiting PROTACs, palbociclib-derived degraders CPs were moderately superior to abemaciclib-derived CP-As, while ribociclib-derived CP-Rs could barely induce CDK6 degradation (Figure S2 and Tables 2 and S1). This may be explained by the distinct binding mode of ribociclib from the other two drugs (Figure 2A). Herein, we discussed PROTAC molecules based on palbociclib and pomalidomide primarily.

To be noted, linker length dependence was observed in CDK6 degraders. PROTACs with shorter linker such as CP-10 and CP-5 possessed higher degradation capacity, which implied these shorter molecules held preferable spatial positions for CRBN recruitment toward CDK6. Moreover, exchanging linker-attaching end at palbociclib side among amide, triazole, and methylene yielded PROTACs with similar degradation potential (DC_{50} of CP-5 of ≈ 1.1 nM, DC_{50} of CP-10 of ≈ 2.1 nM, DC_{50} of CP-15 of ≈ 1.6 nM).

At pomalidomide side, however, degradation potency was decreased by nearly 8-fold when flexible imino group on linkers was replaced by rigid alkyne (DC_{50} of CP-14 of ≈ 10.6 nM, DC_{50} of CP-21 of ≈ 81.6 nM, DC_{50} of CP-22 of ≈ 86.8 nM) but slightly enhanced when imino group was substituted by methylene (DC_{50} of CP-13 of ≈ 5.3 nM, DC_{50} of CP-16 of

Table 2. Structures and DC₅₀ Values for PROTACs Derived from Abemaciclib and Pomalidomide

			
Abemaciclib		CRBN Recruiting	
Compounds	Linker	DC ₅₀ /nM CDK6	DC ₅₀ /nM CDK4
CP-A1		8.6	>500
CP-A2		129.7	>500
CP-A3		271.9	>500
CP-A4		145.5	>500

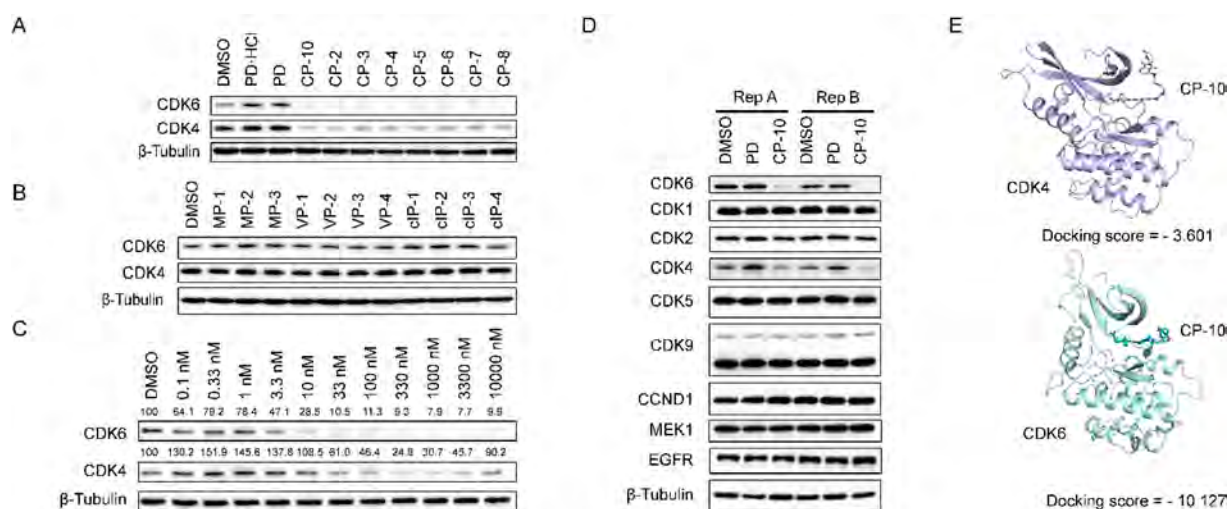


Figure 3. Screen and characterization of potent CDK6-degrading PROTACs. (A, B) CDK6 levels in U251 cells upon 24 h drug treatment. All drugs were administrated at 1 μ M. PD (palbociclib) and PD-HCl (commercialized inhibitor, salt) were applied here as control. (C) CP-10 induced more significant degradation of CDK6 than CDK4. Relative expression levels of CDK4/6 normalized to β -tubulin were labeled. Thus calculated DC₅₀ of CDK6 was about 2.1 nM while DC₅₀ of CDK4 was about 150–180 nM. (D) CP-10 induced specific degradation of CDK6. Shown are immunoblots of representative proteins in samples from two groups of replicates. U251 cells were treated with 500 nM PD, CP-10, or vehicle control (DMSO) for 4 h. (E) Docking of CP-10 onto CDK4 (PDB code 2w96) or CDK6 (PDB code 2euf) via Maestro 11.3 (Schrödinger). Docking scores were presented.

≈ 1.7 nM). These data suggested that CDK6 protein was insensitive to the rotation of linkage moieties near its kinase active pocket, allowing the accession of CRBN from obvious preference of flexible linker due to its narrow binding pocket. We also found that CP-13/14 possessing alkyl linker and CP-15 removing triazole group excelled CP-10 in CDK6 degradation strength, which may result from enhancement of molecule flexibility, hydrophobic solubility, and membrane permeability. Among these CRBN-recruiting PROTACs, CP-10 with the conjugation of palbociclib and pomalidomide

demonstrated the best degradation efficacy with the simplest synthesis procedures (Tables 1, 2, S1). CP-10 induced nearly 72% degradation of CDK6 at 10 nM and 89% at 100 nM in human glioblastoma U251 cells (Figure 3C). The degradation of CDK4 induced by CP-10 was far weaker than that of CDK6 (DC₅₀ 50- to 80-fold) albeit similar to palbociclib affinity and sequence homology of these two kinases (Figure 3C).³¹ Time-lapse analysis showed that CDK6 degradation began at roughly 2 h and was completed by 6 h (Figure S3).

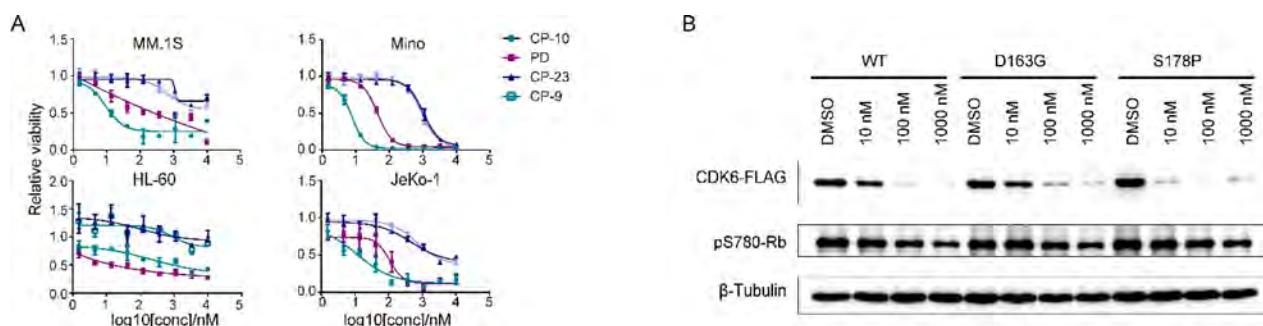


Figure 4. CP-10 inhibited proliferation of cancer cells and induced degradation of amplified/mutated forms of CDK6. (A) A panel of different cancer cells were treated with CP-10/PD/CP-9/CP-23 for 84 h before cell viability measurement by CCK-8. Relative absorbance was plotted. Error bar is SD. (B) CP-10 induced robust degradation of WT, D163G, and S178P forms of CDK6. WT, D163G, and S178P forms of CDK6-FLAG were stably introduced into MCF-7 cells via lentivirus. Cells were then treated as indicated for 24 h before harvesting for immunoblotting. Data were representatives of independent replicate experiments for at least three times.

Control experiments clearly demonstrated that palbociclib, pomalidomide, or unconjugated PROTAC arms could not induce CDK6 degradation (Figure S3). In contrast, palbociclib or pomalidomide could competitively inhibit the degradation effect of CP-10. Additionally, carfilzomib, a proteasome inhibitor, could completely disable the PROTAC effect.³⁴ Strong inhibition was also observed with the neddylation inhibitor MLN-4924, which was in accordance with the requirement of neddylation for processive E3 ligase activity of CRBN³⁵ (Figure S3). The above observations confirmed that degradation of CDK6 was mediated by the ubiquitin–proteasome system.

We also examined the responses of several other CDKs and kinases to CP-10 and found that CP-10 was highly selective for CDK6 without significant off-target effect (Figure 3D). Quantitative proteomic analysis also showed that CDK6 stood out as the most down-regulated protein in the cell upon 4 h CP-10 treatment, further confirming the selectivity of CP-10 for CDK6 (Figure S4A). We did observe several other down-regulated proteins, including ZFP91 and MAP2K7 (MKK7) (Figure S4B). The modest degradation of CDK4 was reasonable because of the high concentration of CP-10 applied. ZFP91 was previously reported to be IMiD-dependent substrate of the CRL4^{CRBN} ubiquitin ligase.³⁶ However, ZFP91 remained unchanged after 24 h CP-10 treatment (Figure S4), indicating that the ZFP91 decrease observed in proteomic analysis was a transient response to high-dose pomalidomide arm. MKK7 also stayed unchanged after 24 h CP-10 incubation, in contrast to the steady and significant degradation of CDK6 (Figure S4).

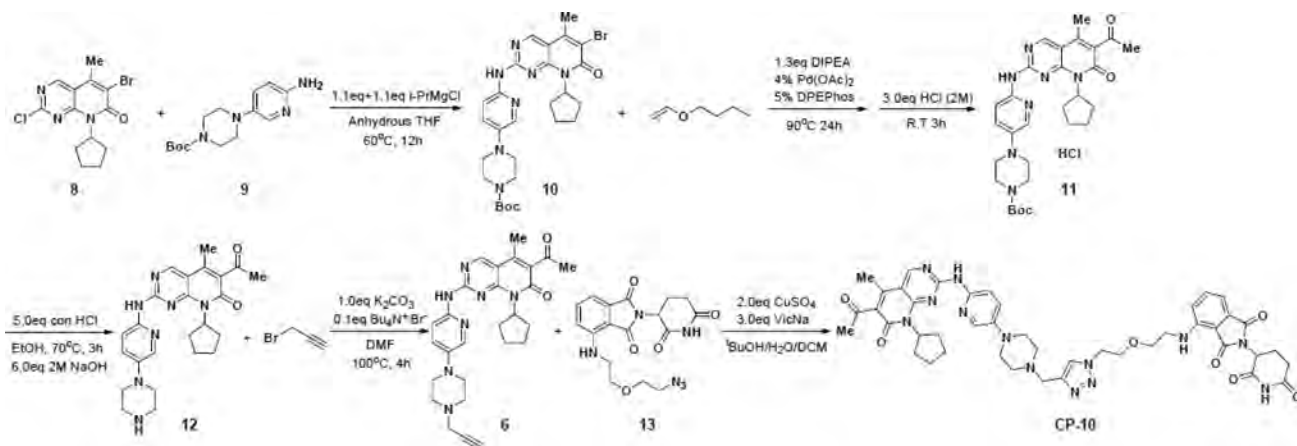
In vitro kinase assay indicated that the kinase inhibitory activity of CP-10 for CDK4 or CDK6 was 10- to 25-fold weaker than that of PD, implying the compromised binding affinity between CP-10 for CDK4 or CDK6 (Figure S4C). Difference in endogenous abundance for both could be ruled out since FLAG-tagged CDK6 was degraded with greater percentage than FLAG-tagged CDK4 when they were expressed at the same level (Figure S4D). The selectivity could be partially explained by the more stable complex formed by CP-10 and CDK6 than CDK4 or by more “match” as displayed by the docking simulation (Figure 3E). The fact that CDK4 has less lysine residues (11 in CDK4 vs 18 in CDK6) for ubiquitination may also contribute to the selectivity, which awaits further exploration. Nonetheless, preferred degradation of CDK6 over CDK4 indicates that PROTAC CP-10 is in a better match for CDK6 than CDK4,

via proper linker and favorable orientation. A stable and “matched” ternary complex of target, E3 ligase, and PROTAC could be formed despite attenuated target-binding affinity.

As CDK6-dependency was claimed mostly in hematopoietic cells,³⁷ we selected several such cell lines to further assess the effect of CP-10 in vitro. Human leukemia cell lines THP-1 and HL-60, human mantle cell lymphoma cell lines Mino and JeKo-1, human multiple myeloma cell lines MM.1S and RPMI8226 were then treated with increasing concentrations of CP-10, and the corresponding inhibition of cell proliferation was evaluated with CCK-8. For control, we also performed parallel experiments with parental drug PD and nondegrading control molecules CP-9 and CP-23. We found that CP-10 displayed a much better cell inhibition potential ($IC_{50} \approx 10$ nM) than PD ($IC_{50} \approx 200$ nM) in multiple myeloma cell MM.1S and mantle cell lymphoma cells (in Mino, CP-10 $IC_{50} \approx 8$ nM, PD $IC_{50} \approx 45$ nM) or comparable activities in leukemia cells (Figure 4A and Figure S5). However, CP-10 was far weaker than PD in another multiple myeloma cell RPMI8226 (Figure S5). As expected, nondegrading PROTACs CP-9 and CP-23 barely inhibited the cell proliferation or at very high concentrations (Figure 4A and Figure S5). Protein levels of CDK4/6 and phospho-Rb (S780), as an indicator of their kinase activities, were in line with the proliferation assay results (Figure S5). These data clearly demonstrated that the inhibition on proliferation by CP-10 was mainly achieved via degradation of target protein instead of residual kinase inhibitory activities. The differential response to CP-10 in multiple cell lines suggested cell context specificity or specific dependence on endogenous CDK4 or CDK6 levels or their ratios. For example, the residual CDK4 proteins upon CP-10 treatment in HL-60 cells probably attenuated the cellular sensitivity to CP-10 compared to PD, and also, indicating that HL-60 cells were not simply dependent on CDK6. We were also surprised to observe the superior potency of CP-10 in MM.1S than pomalidomide and the combination of PD and pomalidomide, as pomalidomide is an approved agent for multiple myeloma treatment (Figure S5). Collectively, these data strongly supported the promising potential of CDK6-degraders in fighting against cancers of hematopoietic origin.

As mentioned in the beginning, the CDK6 overexpression could result in resistance to CDK6 inhibitors in reported preclinical and clinical cases. Therefore, we introduced additional copies of CDK6 into the Ewing’s sarcoma cell line A-673, which expressed scarce CDK6, by lentivirus infection. Indeed, CP-10 cut down the expression levels of overexpressed

Scheme 1. Synthetic Route of Target Compound CP-10



CDK6 (Figure S6). This result indicates that the CDK6-targeting PROTAC degraders may represent a new strategy against CDK6-overexpression induced drug resistance. We tested CP-10 in two independent palbociclib-resistant breast cancer cell lines resulting from CDK6 copy amplification (MCF-7 CDK6N2) and FAT1 loss (MCF-7 FAT1 CR).^{6,7} We found CP-10 could induce degradation of CDK6 and CDK4 and inhibit the proliferation of these palbociclib resistant cell lines (Figure S6).

Moreover, D163G mutation in CDK6 was previously predicted to attenuate palbociclib binding, and S178P was predicted to mimic CDK4 activation and result in CDK6 hyperactivation.^{8,9} Both mutations may lead to clinical resistance for CDK6 inhibitors. As observed, CP-10 induced degradation of these mutants as efficiently as the wild-type CDK6, indicating the robustness for CP-10 induced degradation (Figure 4B). The degradation of CDK6 D163G was a little bit compromised compared to wild type but still significant, suggesting that target binding affinity of palbociclib arm of CP-10 was compromised due to binding hotspot mutation but sufficient to facilitate CDK6 degradation. Again, successful degradation of palbociclib binding site mutant supported the “match” between CP-10 and mutated CDK6 in spite of compromised binding affinity in theory. These preliminary data supported the application potential of overcoming palbociclib resistance via approaches of CDK4/6 degradation.

CONCLUSION

In summary, a focused library of CDK6-degrader was developed and factors including linker length, spatial orientation, and binding affinity were systematically evaluated to help understand the match/mismatch between PROTAC and target and deduce the best strategy for future design or optimization of CDK6 degradation. Remarkably and interestingly, we found that (i) pomalidomide-based PROTACs recruiting CRBN, instead of other tested E3 ligases, resulted in functional degraders; (ii) the dual CDK4/CDK6 ligand palbociclib we applied surprisingly resulted in CDK6 selective PROTACs; (iii) the representative palbociclib-derived PROTAC CP-10 could inhibit proliferation of several hematopoietic cancer cells with impressive potency including multiple myeloma; (iv) mutated and overexpressed CDK6 can still be degraded by CP-10. These data added to the growing trends of potential clinical benefits of PROTAC techniques and also

suggested the specific application of CDK6 degradation in certain cancers.

EXPERIMENTAL SECTION

Chemistry. All reactions were carried out under atmosphere or argon. Glassware was oven-dried prior to use. Unless otherwise indicated, common reagents or materials were obtained from commercial source and used without further purification. Flash column chromatography was performed using silica gel 60 (200–300 mesh). Analytical thin layer chromatography (TLC) was carried out on Yinlong silica gel plates with QF-254 indicator and visualized by UV. The ¹H and ¹³C NMR spectra were recorded at 400 MHz, respectively, on Bruker 400 MHz NMR spectrometer.

All NMR spectra were measured at 25 °C in CDCl₃ or DMSO-*d*₆. Chemical shifts (δ) are reported in parts per million, and coupling constants (*J*) are reported in hertz. The resonance multiplicities in the ¹H NMR spectra are described as “s” (singlet), “d” (doublet), “t” (triplet), “quint” (quintet), and “m” (multiplet), and broad resonances are indicated by “br.” Residual protic solvent of CDCl₃ (¹H, δ 7.26 ppm; ¹³C, δ 77.16 ppm), DMSO-*d*₆ (¹H, δ 2.50 ppm; ¹³C 39.50 ppm) was used as the internal reference in the ¹H and ¹³C NMR spectra. Low-resolution mass spectral analyses were performed with a Waters AQUITY UPLCTM/MS. Purities of the tested compounds, determined by HPLC, were >95%. Preparative HPLC was carried out on 250 mm × 10 mm C-18 column using gradient conditions (1–90% B, flow rate = 3.5 mL/min, 30 min). The eluents used were solvent A (H₂O with 0.1% TFA) and solvent B (CH₃CN with 0.1% TFA).

Synthetic Route of Target Compound CP-10. As shown in Scheme 1, intermediate 12 was prepared according to the patent WO 2014128588 A1.³⁸ First, compound 10 was synthesized via a substitution reaction between 8 and 9 in the presence of isopropylmagnesium chloride. I-PrMgCl was chosen as the base. With this condition, the transformation in step 1, Scheme 1, afforded target product in excellent yield.

Subsequent intermolecular Heck reaction coupled 10 with *n*-butyl vinyl ether followed by acidolysis led to compound 11. The Boc-protecting group of piperazine was then removed under acid condition to afford 12. An alkyne group was introduced to 12 by reacting with propargyl bromide, generating intermediate 6. Finally, the desired degrader CP-10 was obtained through a click reaction coupling the azide group in 13 with the alkyne group in 6.³⁹

6-Acetyl-8-cyclopentyl-5-methyl-2-((5-(4(prop-2-yn-1-yl)piperazin-1-yl)pyridine-2-yl)amino)pyrido[2,3-δ]pyrimidin-7(8H)-one (6). To a solution of palbociclib (500 mg, 1.12 mmol) in DMF were added 3-bromopropyne (106 μL, 1.23 mmol), K₂CO₃ (136 mg, 1.34 mmol), and TBAB (36 mg, 0.11 mmol). The reaction was stirred at 90 °C for 3 h, then washed with water, and the organic layer was concentrated to dryness. Flash column chromatography (CH₂Cl₂/MeOH, 40:1, vol/vol) gave compound 9 (438 mg, 81%) as

yellow solid. $R_f = 0.4$, $\text{CH}_2\text{Cl}_2/\text{MeOH}$ 20:1; ^1H NMR (400 MHz, CDCl_3) δ 8.83 (s, 1H), 8.38 (s, 1H), 8.16 (d, $J = 9.0$ Hz, 1H), 8.07 (d, $J = 2.8$ Hz, 1H), 7.33 (dd, $J^1 = 9.1$ Hz, $J^2 = 3.0$ Hz, 1H), 5.92–5.83 (m, 1H), 3.39 (d, $J = 2.4$ Hz, 2H), 3.24 (t, $J = 4.8$ Hz, 4H), 2.77 (t, $J = 4.8$ Hz, 4H), 2.54 (s, 3H), 2.37 to 2.33 (m, 5H), 2.29 (t, $J = 2.4$ Hz, 1H), 2.07–2.04 (m, 2H), 1.92 to 1.85 (m, 2H), 1.70–1.66 (m, 2H); ^{13}C NMR (400 MHz, CDCl_3) δ 202.84, 161.59, 158.25, 157.40, 155.70, 145.09, 143.73, 14.95, 136.81, 130.87, 126.06, 113.76, 107.88, 78.55, 73.70, 54.19, 51.78, 49.54, 47.07, 31.70, 28.23, 25.91, 14.12, 8.23. LC–MS (ESI⁺): m/z calculated for $\text{C}_{27}\text{H}_{31}\text{N}_7\text{O}_2$, 486.25 $[\text{M} + \text{H}]^+$; found 487.6194.

4-((2-(4-((6-((6-Acetyl-8-cyclopentyl-5-methyl-7-oxo-7,8-dihydropyrido[2,3-*d*]pyrimidin-2-yl)amino)pyridin-3-yl)-piperazin-1-yl)methyl)-1*H*-1,2,3-triazol-1-yl)ethoxy)ethyl)-amino)-2-(2,6-dioxopiperidin-3-yl)isoindoline-1,3-dione (CP-10). Compound 6 (15 mg, 0.03 mmol), compound 13 (0.04 mmol, 1.2 equiv), and sodium ascorbate (17.8 mg, 0.09 mmol) were dissolved in BuOH/DCM , 1 mL/0.5 mL, and then a solution of CuSO_4 (9.6 mg, 0.06 mmol) in 0.5 mL of water was added. The resulting mixture was stirred at room temperature for 10 min. After the reaction was completed, the solvent was removed and then dealt with 7 M ammonium hydroxide. The organic layer was separated and concentrated to dryness. Flash column chromatography ($\text{CH}_2\text{Cl}_2/\text{MeOH}$, 20:1, vol/vol) gave compound CP-10 (0.019 mmol, 63%) as solid. $R_f = 0.4$, $\text{CH}_2\text{Cl}_2/\text{MeOH}$ 10:1. ^1H NMR (400 MHz, CDCl_3) δ 10.34 (s, 1H), 8.79 (s, 1H), 8.22 (s, 1H), 8.12 (d, $J = 9.1$ Hz, 1H), 8.02 (d, $J = 2.5$ Hz, 1H), 7.75 (s, 1H), 7.51 (dd, $J^1 = 8.3$ Hz, $J^2 = 7.3$ Hz, 1H), 7.30 (dd, $J^1 = 9.1$ Hz, $J^2 = 2.5$ Hz, 1H), 7.14 (d, $J = 7.3$ Hz, 1H), 6.90 (d, $J = 8.3$ Hz, 1H), 6.63 (t, $J = 5.3$ Hz, 1H), 5.89–5.84 (m, 1H), 4.92–4.88 (m, 1H), 4.60–4.60 (m, 2H), 3.94–3.87 (m, 3H), 3.72–3.63 (m, 3H), 3.43–3.41 (m, 2H), 3.24–3.19 (m, 4H), 2.76–2.69 (m, 7H), 2.54 (s, 3H), 2.36–2.32 (m, 5H), 2.19–2.15 (m, 1H), 2.07–2.03 (m, 2H), 1.89–1.83 (m, 2H), 1.70–1.66 (m, 2H); ^{13}C NMR (400 MHz, CDCl_3) δ 202.87, 712.18, 169.99, 169.54, 167.62, 161.58, 158.25, 157.39, 155.68, 147.07, 141.99, 136.42, 132.69, 130.81, 126.09, 124.75, 117.17, 112.30, 110.93, 107.79, 77.39, 69.91, 69.61, 68.12, 54.23, 52.84, 52.49, 50.67, 49.18, 49.06, 42.40, 31.69, 31.55, 29.84, 28.20, 27.06, 25.87, 25.76, 23.20, 14.10. LC–MS (ESI⁺): m/z calculated for $\text{C}_{44}\text{H}_{49}\text{N}_{13}\text{O}_7$, 437.195 $[\text{M} + 2\text{H}]^{2+}$; found 437.2669. Purities of CP-10 determined by HPLC were >95% (shown in Supporting Information).

■ ASSOCIATED CONTENT

Supporting Information

The Supporting Information is available free of charge on the ACS Publications website at DOI: 10.1021/acs.jmedchem.9b00871.

Details for synthesis routines, HPLC analysis, predictive model construction and biological experiments, supplementary figures and tables, and abbreviations used in this article (PDF)

Molecular formula strings and some data (CSV)

■ AUTHOR INFORMATION

Corresponding Authors

*W.W.: e-mail, wwwu@tsinghua.edu.cn.

*Y.R.: e-mail, yrao@tsinghua.edu.cn.

ORCID

Shang Su: 0000-0003-0228-5380

Yu Rao: 0000-0002-4356-8531

Author Contributions

[†]S.S. and Z.Y. contributed equally. All authors have given approval to the final version of the manuscript.

Notes

The authors declare the following competing financial interest(s): S.C. has received research support (to institution)

from Genentech, Novartis, Eli Lilly, Daiichi Sankyo, and Sanofi and ad hoc consulting fees (to S.C.) from Eli Lilly, Novartis, Sermonix, Revolution Medicines, Context Therapeutics, and BMS. All the other authors declare no conflicts of interest.

■ ACKNOWLEDGMENTS

We thank Dr. Jiahui Han and Dr. Wensheng Wei for sharing reagents. We also thank Dr. Haitao Li, Dr. Qiaoran Xi, Dr. Xiaonan Su, Dr. Xiuyun Sun, Ye Sun, and Dan Wang for helpful discussions and suggestions and Dr. Libing Mu for cartoon illustration assistance. Y.R.'s research is funded by National Natural Science Foundation of China (Grants 81573277, 81622042, 81773567) and National Major Scientific and Technological Special Project for "Significant New Drugs Development" (Grant SQ2017ZX095003). W.W.'s research was funded by National Natural Science Foundation of China (Grant 81672950). S.C.'s research is funded by NIH Cancer Center Support Grant (CCSG) P30 CA08748 and the Breast Cancer Research Foundation.

■ REFERENCES

- (1) Vermeulen, K.; Van Bockstaele, D. R.; Berneman, Z. N. The cell cycle: a review of regulation, deregulation and therapeutic targets in cancer. *Cell Proliferation* **2003**, *36*, 131–149.
- (2) Otto, T.; Sicinski, P. Cell cycle proteins as promising targets in cancer therapy. *Nat. Rev. Cancer* **2017**, *17*, 93–115.
- (3) Tadesse, S.; Yu, M.; Kumarasiri, M.; Le, B. T.; Wang, S. Targeting CDK6 in cancer: state of the art and new insights. *Cell Cycle* **2015**, *14*, 3220–3230.
- (4) Niesvizky, R.; Badros, A. Z.; Costa, L. J.; Ely, S. A.; Singhal, S. B.; Stadtmauer, E. A.; Haideri, N. A.; Yacoub, A.; Hess, G.; Lentzsch, S.; Spicka, I.; Chanan-Khan, A. A.; Raab, M. S.; Tarantolo, S.; Vij, R.; Zonder, J. A.; Huang, X.; Jayabalan, D.; Di Liberto, M.; Huang, X.; Jiang, Y.; Kim, S. T.; Randolph, S.; Chen-Kiang, S. Phase 1/2 study of cyclin-dependent kinase (CDK)4/6 inhibitor palbociclib (PD-0332991) with bortezomib and dexamethasone in relapsed/refractory multiple myeloma. *Leuk. Lymphoma* **2015**, *56*, 3320–3328.
- (5) National Cancer Institute. Clinical trials using palbociclibpage. <https://www.cancer.gov/about-cancer/treatment/clinical-trials/intervention/palbociclib> (accessed Mar 29, 2019).
- (6) Yang, C.; Li, Z.; Bhatt, T.; Dickler, M.; Giri, D.; Scaltriti, M.; Baselga, J.; Rosen, N.; Chandarlapaty, S. Acquired CDK6 amplification promotes breast cancer resistance to CDK4/6 inhibitors and loss of ER signaling and dependence. *Oncogene* **2017**, *36*, 2255–2264.
- (7) Li, Z.; Razavi, P.; Li, Q.; Toy, W.; Liu, B.; Ping, C.; Hsieh, W.; Sanchez-Vega, F.; Brown, D. N.; Da Cruz Paula, A. F.; Morris, L.; Selenica, P.; Eichenberger, E.; Shen, R.; Schultz, N.; Rosen, N.; Scaltriti, M.; Brogi, E.; Baselga, J.; Reis-Filho, J. S.; Chandarlapaty, S. Loss of the FAT1 tumor suppressor promotes resistance to CDK4/6 inhibitors via the Hippo pathway. *Cancer Cell* **2018**, *34*, 893–905.
- (8) Bockstaele, L.; Bisteau, X.; Paternot, S.; Roger, P. P. Differential regulation of cyclin-dependent kinase 4 (CDK4) and CDK6, evidence that CDK4 might not be activated by CDK7, and design of a CDK6 activating mutation. *Mol. Cell. Biol.* **2009**, *29*, 4188–4200.
- (9) Hernandez Maganhi, S.; Jensen, P.; Caracelli, I.; Zukerman Schpector, J.; Frohling, S.; Friedman, R. Palbociclib can overcome mutations in cyclin dependent kinase 6 that break hydrogen bonds between the drug and the protein. *Protein Sci.* **2017**, *26*, 870–879.
- (10) Neklesa, T. K.; Winkler, J. D.; Crews, C. M. Targeted protein degradation by PROTACs. *Pharmacol. Ther.* **2017**, *174*, 138–144.
- (11) Ottis, P.; Toure, M.; Cromm, P. M.; Ko, E.; Gustafson, J. L.; Crews, C. M. Assessing different E3 Ligases for small molecule induced protein ubiquitination and degradation. *ACS Chem. Biol.* **2017**, *12*, 2570–2578.

- (12) Lai, A. C.; Crews, C. M. Induced protein degradation: an emerging drug discovery paradigm. *Nat. Rev. Drug Discovery* **2017**, *16*, 101–114.
- (13) Sakamoto, K. M.; Kim, K. B.; Kumagai, A.; Mercurio, F.; Crews, C. M.; Deshaies, R. J. Protacs: chimeric molecules that target proteins to the Skp1-Cullin-F box complex for ubiquitination and degradation. *Proc. Natl. Acad. Sci. U. S. A.* **2001**, *98*, 8554–8559.
- (14) Burslem, G. M.; Smith, B. E.; Lai, A. C.; Jaime-Figueroa, S.; McQuaid, D. C.; Bondeson, D. P.; Toure, M.; Dong, H.; Qian, Y.; Wang, J.; Crew, A. P.; Hines, J.; Crews, C. M. The advantages of targeted protein degradation over inhibition: An RTK Case Study. *Cell Chem. Biol.* **2018**, *25*, 67–77.
- (15) Winter, G. E.; Buckley, D. L.; Paulk, J.; Roberts, J. M.; Souza, A.; Dhe-Paganon, S.; Bradner, J. E. Drug Development. Phthalimide conjugation as a strategy for in vivo target protein degradation. *Science* **2015**, *348*, 1376–1381.
- (16) Lu, J.; Qian, Y.; Altieri, M.; Dong, H.; Wang, J.; Raina, K.; Hines, J.; Winkler, J. D.; Crew, A. P.; Coleman, K.; Crews, C. M. Hijacking the E3 ubiquitin ligase cereblon to efficiently target BRD4. *Chem. Biol.* **2015**, *22*, 755–763.
- (17) Sun, Y.; Zhao, X.; Ding, N.; Gao, H.; Wu, Y.; Yang, Y.; Zhao, M.; Hwang, J.; Song, Y.; Liu, W.; Rao, Y. PROTAC-induced BTK degradation as a novel therapy for mutated BTK C481S induced ibrutinib-resistant B-cell malignancies. *Cell Res.* **2018**, *28*, 779–781.
- (18) Zhao, Q.; Lan, T.; Su, S.; Rao, Y. Induction of apoptosis in MDA-MB-231 breast cancer cells by a PARP1-targeting PROTAC small molecule. *Chem. Commun.* **2019**, *55*, 369–372.
- (19) An, Z.; Lv, W.; Su, S.; Wu, W.; Rao, Y. Developing potent PROTACs tools for selective degradation of HDAC6 protein. *Protein Cell* **2019**, *10*, 606–609.
- (20) Jiang, B.; Wang, E. S.; Donovan, K. A.; Liang, Y.; Fischer, E. S.; Zhang, T.; Gray, N. S. Development of dual and selective degraders of cyclin-dependent kinases 4 and 6. *Angew. Chem., Int. Ed.* **2019**, *58*, 6321–6326.
- (21) Hatcher, J. M.; Wang, E. S.; Johannessen, L.; Kwiatkowski, N.; Sim, T.; Gray, N. S. Development of highly potent and selective steroidal inhibitors and degraders of CDK8. *ACS Med. Chem. Lett.* **2018**, *9*, 540–545.
- (22) Olson, C. M.; Jiang, B.; Erb, M. A.; Liang, Y.; Doctor, Z. M.; Zhang, Z.; Zhang, T.; Kwiatkowski, N.; Boukhali, M.; Green, J. L.; Haas, W.; Nomanbhoy, T.; Fischer, E. S.; Young, R. A.; Bradner, J. E.; Winter, G. E.; Gray, N. S. Pharmacological perturbation of CDK9 using selective CDK9 inhibition or degradation. *Nat. Chem. Biol.* **2018**, *14*, 163–170.
- (23) Bondeson, D. P.; Mares, A.; Smith, I. E.; Ko, E.; Campos, S.; Miah, A. H.; Mulholland, K. E.; Routly, N.; Buckley, D. L.; Gustafson, J. L.; Zinn, N.; Grandi, P.; Shimamura, S.; Bergamini, G.; Faeltsh-Savitski, M.; Bantscheff, M.; Cox, C.; Gordon, D. A.; Willard, R. R.; Flanagan, J. J.; Casillas, L. N.; Votta, B. J.; den Besten, W.; Famm, C.; Kruidenier, L.; Carter, P. S.; Harling, J. D.; Churcher, I.; Crews, C. M. Catalytic in vivo protein knockdown by small-molecule PROTACs. *Nat. Chem. Biol.* **2015**, *11*, 611–617.
- (24) Crew, A. P.; Raina, K.; Dong, H.; Qian, Y.; Wang, J.; Vigil, D.; Serebrenik, Y. V.; Hamman, B. D.; Morgan, A.; Ferraro, C.; Siu, K.; Neklesa, T. K.; Winkler, J. D.; Coleman, K. G.; Crews, C. M. Identification and characterization of Von Hippel-Lindau-recruiting proteolysis targeting chimeras (PROTACs) of TANK-Binding Kinase 1. *J. Med. Chem.* **2018**, *61*, 583–598.
- (25) Cromm, P. M.; Samarasinghe, K. T. G.; Hines, J.; Crews, C. M. Addressing kinase-independent functions of Fak via PROTAC-mediated degradation. *J. Am. Chem. Soc.* **2018**, *140*, 17019–17026.
- (26) Smith, B. E.; Wang, S. L.; Jaime-Figueroa, S.; Harbin, A.; Wang, J.; Hamman, B. D.; Crews, C. M. Differential PROTAC substrate specificity dictated by orientation of recruited E3 ligase. *Nat. Commun.* **2019**, *10*, 131.
- (27) Buhimschi, A. D.; Armstrong, H. A.; Toure, M.; Jaime-Figueroa, S.; Chen, T. L.; Lehman, A. M.; Woyach, J. A.; Johnson, A. J.; Byrd, J. C.; Crews, C. M. Targeting the C481S ibrutinib-resistance mutation in Bruton's Tyrosine Kinase using PROTAC-mediated degradation. *Biochemistry* **2018**, *57*, 3564–3575.
- (28) Salami, J.; Alabi, S.; Willard, R. R.; Vitale, N. J.; Wang, J.; Dong, H.; Jin, M.; McDonnell, D. P.; Crew, A. P.; Neklesa, T. K.; Crews, C. M. Androgen receptor degradation by the proteolysis-targeting chimera ARCC-4 outperforms enzalutamide in cellular models of prostate cancer drug resistance. *Commun. Biol.* **2018**, *1*, 100.
- (29) Lai, A. C.; Toure, M.; Hellerschmied, D.; Salami, J.; Jaime-Figueroa, S.; Ko, E.; Hines, J.; Crews, C. M. Modular PROTAC design for the degradation of oncogenic BCR-ABL. *Angew. Chem., Int. Ed.* **2016**, *55*, 807–810.
- (30) Sherr, C. J.; Beach, D.; Shapiro, G. I. Targeting CDK4 and CDK6: from discovery to therapy. *Cancer Discovery* **2016**, *6*, 353–67.
- (31) Chen, P.; Lee, N. V.; Hu, W.; Xu, M.; Ferre, R. A.; Lam, H.; Bergqvist, S.; Solowiej, J.; Diehl, W.; He, Y. A.; Yu, X.; Nagata, A.; VanArsdale, T.; Murray, B. W. Spectrum and degree of CDK drug interactions predicts clinical performance. *Mol. Cancer Ther.* **2016**, *15*, 2273–2281.
- (32) Lu, H.; Schulze-Gahmen, U. Toward understanding the structural basis of cyclin-dependent kinase 6 specific inhibition. *J. Med. Chem.* **2006**, *49*, 3826–3831.
- (33) Toure, M.; Crews, C. M. Small-molecule PROTACS: New approaches to protein degradation. *Angew. Chem., Int. Ed.* **2016**, *55*, 1966–1973.
- (34) Kuhn, D. J.; Chen, Q.; Voorhees, P. M.; Strader, J. S.; Shenk, K. D.; Sun, C. M.; Demo, S. D.; Bennett, M. K.; van Leeuwen, F. W.; Chanan-Khan, A. A.; Orłowski, R. Z. Potent activity of carfilzomib, a novel, irreversible inhibitor of the ubiquitin-proteasome pathway, against preclinical models of multiple myeloma. *Blood* **2007**, *110*, 3281–3290.
- (35) Nawrocki, S. T.; Griffin, P.; Kelly, K. R.; Carew, J. S. MLN4924: a novel first-in-class inhibitor of NEDD8-activating enzyme for cancer therapy. *Expert Opin. Invest. Drugs* **2012**, *21*, 1563–1573.
- (36) An, J.; Ponthier, C. M.; Sack, R.; Seebacher, J.; Stadler, M. B.; Donovan, K. A.; Fischer, E. S. pSILAC mass spectrometry reveals ZFP91 as IMiD-dependent substrate of the CRL4CRBN ubiquitin ligase. *Nat. Commun.* **2017**, *8*, 15398.
- (37) Kim, S.; Tiedt, R.; Loo, A.; Horn, T.; Delach, S.; Kovats, S.; Haas, K.; Engstler, B. S.; Cao, A.; Pinzon-Ortiz, M.; Mulford, I.; Acker, M. G.; Chopra, R.; Brain, C.; di Tomaso, E.; Sellers, W. R.; Caponigro, G. The potent and selective cyclin-dependent kinases 4 and 6 inhibitor ribociclib (LEE011) is a versatile combination partner in preclinical cancer models. *Oncotarget* **2018**, *9*, 35226–35240.
- (38) Chekal, B. P.; Ide, N. D. Solid forms of a selective cdk4/6 inhibitor. WO Patent 2014128588 A1, Aug 28, 2014.
- (39) Wurz, R. P.; Dellamaggiore, K.; Dou, H.; Javier, N.; Lo, M. C.; McCarter, J. D.; Mohl, D.; Sastri, C.; Lipford, J. R.; Cee, V. J. A “Click chemistry platform” for the rapid synthesis of bispecific molecules for inducing protein degradation. *J. Med. Chem.* **2018**, *61*, 453–461.